

Kinetic study of ignition of Mg/NaNO₃ pyrotechnic using non-isothermal TG/DSC technique

H. R. Pouretedal · M. Ravanbod

Received: 23 April 2014 / Accepted: 23 November 2014 / Published online: 24 December 2014
© Akadémiai Kiadó, Budapest, Hungary 2014

Abstract The non-isothermal TG/DSC technique has been used to study the kinetic triplet of ignition reaction of Mg/NaNO₃ pyrotechnic under nitrogen atmosphere at different heating rates (5, 10, 15, and 20 °C min⁻¹). The TG/DSC results showed that the mass gain after ignition increased and the heat of ignition reaction decreased with increasing heating rate, indicating that the reaction between Mg and NaNO₃ was not complete during the ignition process. The activation energy (E_a) was calculated using Starink model-free method. The pre-exponential factor (A) and kinetic model function were determined by means of the compensation effect and the selected model was confirmed by the nonlinear model fitting method. The average values of E_a and $\log A$ for the ignition reaction of Mg/NaNO₃ were found to be 148.46 ± 3.37 kJ mol⁻¹ and 10.04 min⁻¹, respectively. The model fitting method proved that the ignition reaction of Mg/NaNO₃ pyrotechnic follows the mechanism of A₄ ($g(x) = [-\ln(1-x)]^{1/4}$) as a nucleation reaction model.

Keywords Pyrotechnic · Thermal ignition · Non-isothermal · Kinetic triplet

Introduction

A pyrotechnic composition is usually a homogenized mixture of small particles of organic or inorganic oxidizers

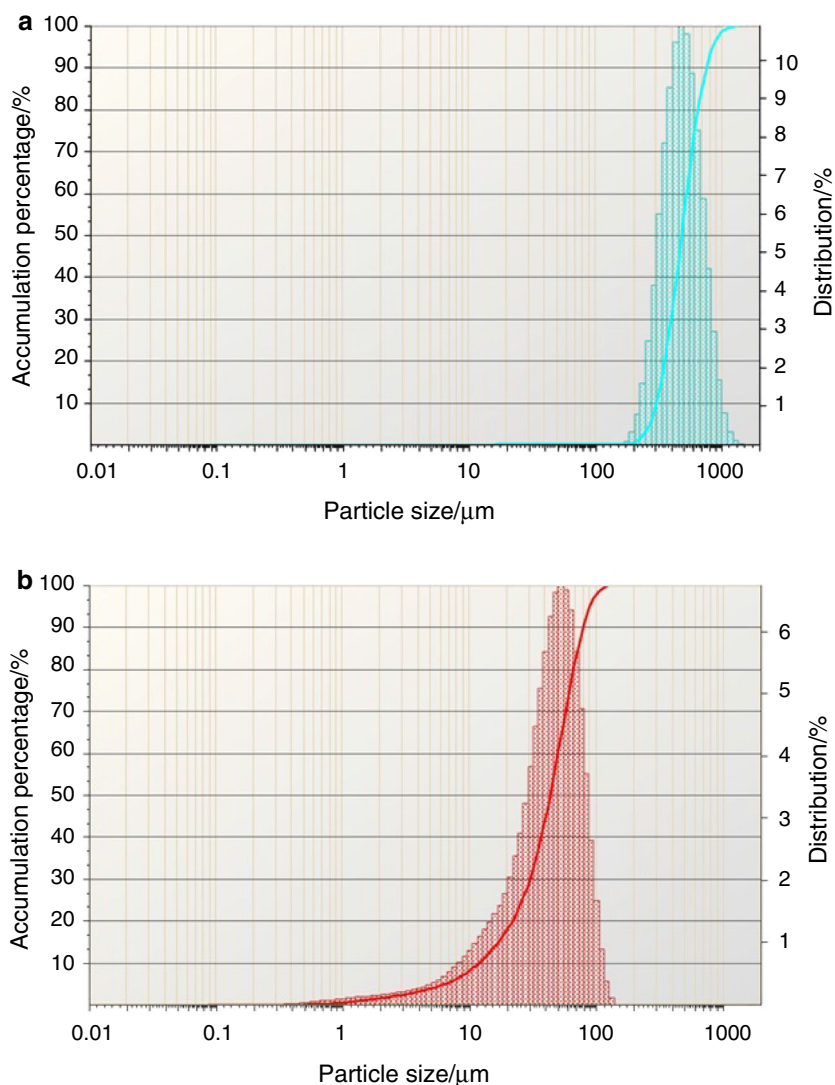
and fuels designed to produce heat, light, sound, smoke, or combination of these through self-sustaining exothermic reactions that do not rely on oxygen from external sources. The oxidizers are usually oxygen-rich ionic solids which are used in pyrotechnic composition to facilitate the process of ignition by producing oxygen [1]. Sodium nitrate (NaNO₃) has long been a main oxidizer in many pyrotechnics [2]. Magnesium (Mg) powder is a common combustible material in pyrotechnic formulations [3–6]. Due to its excellent light-emitting properties, high exothermicity, easy and stable ignition, magnesium has been widely used in flash agents, illuminating agents, flare agents, fireworks, etc. [7].

There are many reasons why the mechanism and kinetics of thermal ignition of energetic materials are so important for the military industry. From a practical point of view, the rate of thermal ignition is the most important property in characterizing the quality of an energetic material and its shelf life, as well as its thermal hazard potential. In order to predict the shelf life and thermal hazard potential of an energetic material with required accuracy, true ignition mechanism and kinetic constants should be known [8].

Thermal analysis methods play an important role in the study of pyrotechnic reactions, because they thermally simulate the conditions in the propagation wave by following the reactions at high temperature [9]. Due to high sensitivity, a differential scanning calorimeter (DSC) can provide detailed information on the mechanism of ignition reactions [10, 11]. Among the several methods of analysis of DSC data, the isoconversional method has been recommended as a trustworthy way for determining reliable and consistent activation energies ($E_{a,s}$) of solid-state reactions [12]. In fact, the isoconversional methods can determine the actual value of E_a from DSC data without knowledge of the kinetic model [13–16].

H. R. Pouretedal (✉) · M. Ravanbod
Faculty of Applied Chemistry, Malek-ashtar University of
Technology, Shahin-Shahr, Iran
e-mail: hr_pouretedal@mut-es.ac.ir

Fig. 1 Particle size distribution of **a** Mg powder ($D_{50} = 483 \mu\text{m}$) and **b** NaNO_3 powder ($D_{50} = 43.7 \mu\text{m}$)



The aim of this work was to study the endothermic or exothermic changes of Mg/NaNO_3 pyrotechnic mixture heated in nitrogen atmosphere through TG/DSC measurements and to obtain some information on characteristic ignition temperatures and after ignition processes. To the best of our knowledge there is no report on the kinetic triple of ignition and after ignition reaction of Mg/NaNO_3 (50/50) pyrotechnic mixture. Ostmark and Roman investigated Mg/NaNO_3 (58/42) pyrotechnic mixture using laser ignition method and reported activation energy and pre-exponential factor [17]. They have not reported the reaction model and after ignition processes. Rao and Singh studied the burning rate characteristics of Mg/NaNO_3 at different mixture ratios and particle sizes. Their investigation indicated that the compositions containing finer particle size (50 μm) NaNO_3 gave higher burning

rate at high fuel content of the mixture than at the stoichiometric ratio [18]. The luminosity and burn rate of Mg/NaNO_3 compositions with epoxy resin were studied by Palaiah et al. [19]. According to their report, high luminous efficiency is achieved for the composition based on magnesium/sodium nitrate ratio 70/30 with 4 % epoxy resin.

The ICTAC kinetic committee recommendations [20] were used for reliable estimation of kinetic parameters including activation energy and pre-exponential factor, and determination of the reaction model for thermal ignition of the pyrotechnic composition. The activation energy for the ignition process was calculated by Starink method based on DSC data at different heating rates. Then the compensation effect method was used for accurate determination of the reaction model and pre-exponential factor.

Experimental

Analytical grade sodium nitrate (purity >99 %) and magnesium powder (purity >99 %) were purchased from Merck Company and Tangshan Weihao Magnesium powder Co. Ltd, respectively. Sodium nitrate was ground in a mortar to produce a fine powder and then dried at 80 °C for 2 h. The particle size distribution of magnesium and sodium nitrate powders are shown in Fig. 1. The particles size of sodium nitrate and magnesium powders are seen about in the range of 1–100 and 300–1,000 μm and the median (D₅₀) of particles size are 43.7 and 483 μm, respectively.

A mixture of fuel-rich Mg/NaNO₃ (50/50) was prepared by intimately mixing the powders in a mortar for about 15 min.

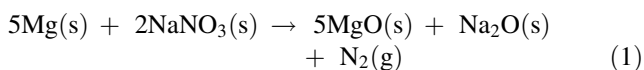
TG–DSC measurements were carried out using a Perkin Elmer simultaneous thermal analyzer model STA 6000 (USA). Alumina sample vessels were used (70 μL volume) with alumina powder as the reference material. Nitrogen atmosphere was applied during the analysis (flow rate of 50 mL min⁻¹). For kinetic study of the reactions, experiments were performed at different heating rates of 5, 10, 15, and 20 °C min⁻¹. In each experiment, approximately 2 mg of Mg/NaNO₃ pyrotechnic mixture was heated from ambient temperature (25 °C) to 800 °C.

The particle size distribution tests were performed using a laser particle size analyzer (FRITTSCH, model Analysette 22, Micro Tec Plus).

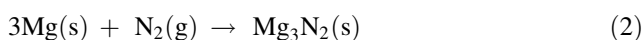
Results and discussion

TG curves of Mg/NaNO₃ mixture

The TG curves in Fig. 2 show typical mass changes as a function of temperature for the Mg/NaNO₃ (50/50) powder mixture heated at different heating rates (5, 10, 15, and 20 °C min⁻¹) under nitrogen atmosphere. The TG curves show two mass losses; one above the melting temperature (*T_m*) to about 450 °C that can be due to the formation of little nitrite [21]. The second sharp mass loss occurs due to release of N₂ gas at the ignition point between magnesium and sodium nitrate according to reaction (1) [22]:



Note that the TG curves show mass gain after the ignition point, probably due to nitridation of the unreacted Mg under nitrogen atmosphere at high temperature according to reaction (2) [23]:



Based on TG curves, the mass loss at ignition points slightly decreases, but the after ignition mass gain considerably increases by increasing the heating rate. These results suggest that the reaction between NaNO₃ and Mg was not complete during the ignition process.

DSC curves of Mg/NaNO₃ mixture

Figure 3 shows the DSC curves of Mg/NaNO₃ (50–50) mixture obtained under different heating rates (5, 10, 15, and 20 °C min⁻¹) under nitrogen atmosphere. The endothermic peak observed around 306 °C in all four DSC curves can be assigned to melting point of sodium nitrate [24, 25]. As the heating rates increase, the exothermic peaks for the ignition process shift to higher temperatures (470.6, 490.2, 502.6, and 511.7 °C, for heating rates of 5, 10, 15, and 20 °C min⁻¹, respectively) and the corresponding heats of reaction decrease from 5,583 to 5,042, 4,490, and 4,150 J g⁻¹. The results, in agreement with those of TG curves, indicate that the reaction between NaNO₃ and Mg is less complete with the increasing heating rates, and there is insufficient time for the complete reaction to occur.

Figure 4 shows the conversion–temperature (*α*–*T*) curves at different heating rates for thermal ignition of Mg/NaNO₃ mixture. The *α*–*T* curves at all heating rates show the same sigmoidal shapes. It can help to verify the validity of predicted reaction model of Avrami–Erofeev or Prout–Tompkins [26].

Kinetic of solid-state reactions

The rate of processes in solid-state is generally a function of temperature and conversion, which can be described by the following equation:

$$\frac{d\alpha}{dt} = k(T) \cdot f(\alpha), \quad (3)$$

where *α* is the conversion fraction, *t* is time, *T* is absolute temperature (*K*), and *f*(*α*) is the reaction model function depending on the particular decomposition mechanism. The temperature function *k*(*T*) is the “rate constant”, representing the temperature dependence of the reaction rate. The *k*(*T*) is usually represented by Arrhenius relationship as:

$$k(T) = A \cdot \exp\left[\frac{-E_a}{RT}\right], \quad (4)$$

where *E_a* is the activation energy as a function of *α* (kJ mol⁻¹), *R* is the universal gas constant (8.314 J mol⁻¹ K⁻¹), and *A* (min⁻¹) is the pre-exponential (frequency) factor which is assumed to be independent of

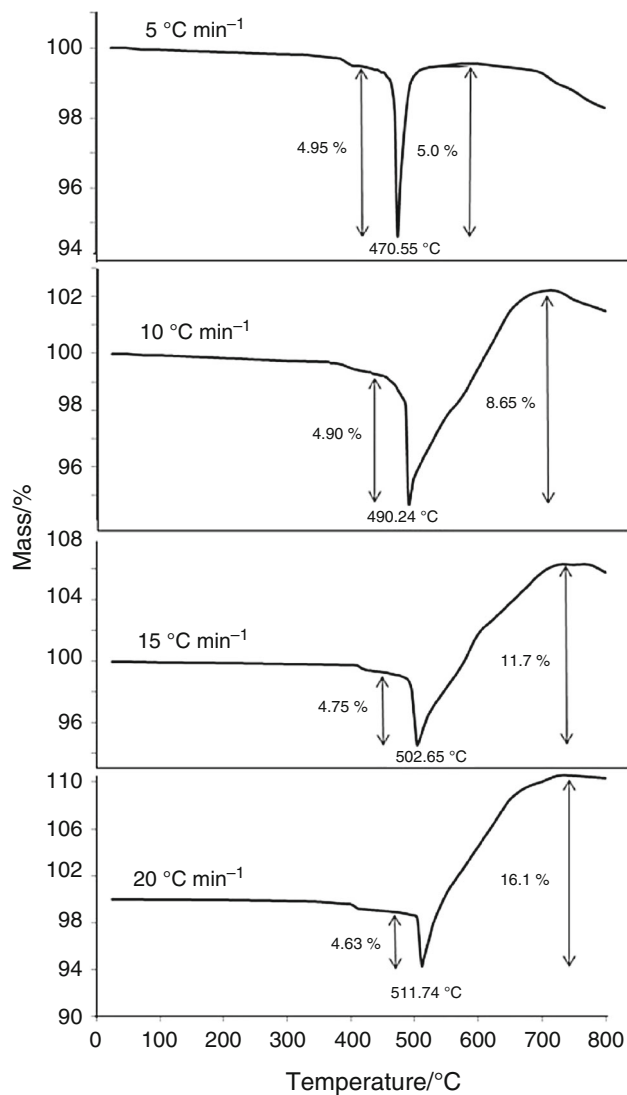


Fig. 2 TG curves for Mg/NaNO₃ (50/50) at different heating rates in N₂ atmosphere

temperature and gives an idea of the association tendency of reacting molecules [27].

The parameters E_a , A , and $f(\alpha)$ are called the kinetic triplet, which is required for prediction of the thermal stability of the materials at various temperatures [28, 29] and needed to provide mathematical description of the process [30].

Calculation of activation energy by model-free isoconversional method

The Starink method [31] was used to determine the activation energy of the ignition reaction of Mg/NaNO₃ pyrotechnic based on conversion fraction of DSC peak area. This method can be expressed by the following equation:

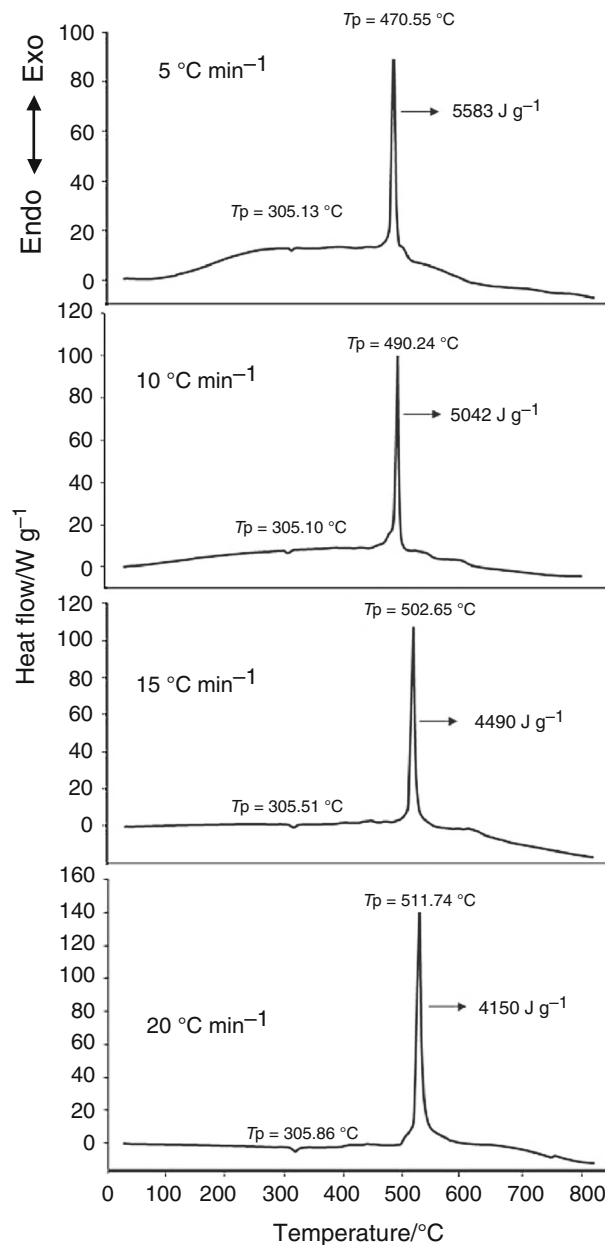


Fig. 3 DSC curves for Mg/NaNO₃ (50/50) at different heating rates in N₂ atmosphere

$$\ln\left(\frac{\beta}{T^{1.92}}\right) = \text{Const} - 1.0008\left(\frac{E_a}{RT}\right). \quad (5)$$

According to the above-mentioned equation, the plots of $\ln(\beta/T^{1.92})$ versus $1/T$ corresponding to different extents of conversion, α , can be obtained by linear regression using least squares method. The activation energy (E_a) can be evaluated from the slope of the straight line which gives the best regression coefficients (R^2). The activation energies were calculated at heating rates of 5, 10, 15, and 20 °C min⁻¹ via these methods for different α values in the range 0.1–0.9.

Fig. 4 α - T Curves at different heating rates for thermal ignition of Mg/NaNO₃

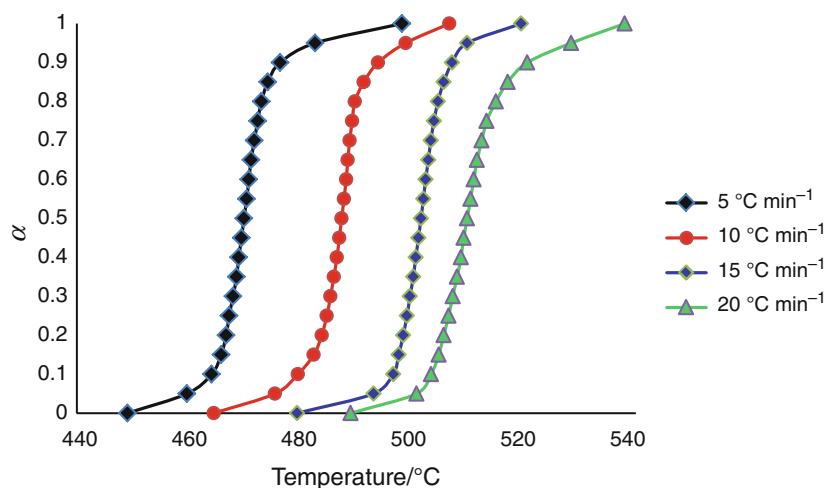


Fig. 5 Starink plots for ignition process of Mg/NaNO₃ mixture at four heating rates and various conversions ($\alpha = 0.1$ – 0.9 , with 0.1 increment)

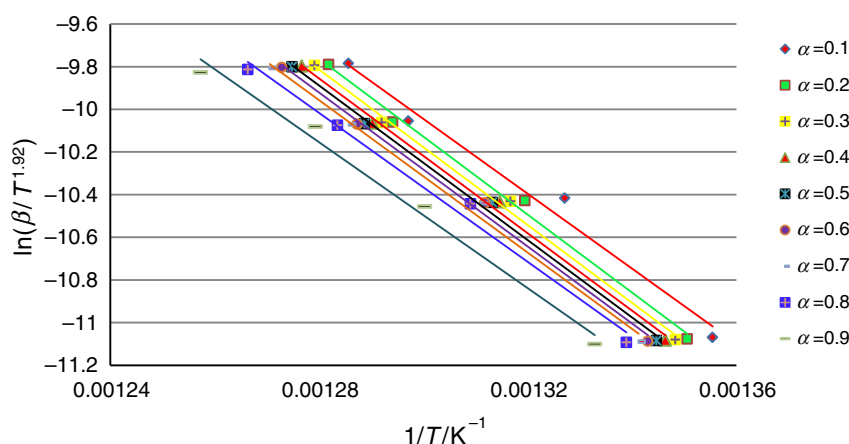


Table 1 The activation energy (E_a) calculated by Starink method for the ignition reaction of Mg/NaNO₃ at α value of 0.1–0.9

α	$E_a/\text{kJ mol}^{-1}$	R^2
0.1	145.80	0.982
0.2	151.78	0.995
0.3	151.53	0.996
0.4	150.79	0.996
0.5	150.50	0.996
0.6	150.00	0.995
0.7	148.54	0.993
0.8	145.03	0.990
0.9	142.15	0.988
Average	148.46 ± 3.37	0.992

The results of analysis by the Starink method from four DSC measurements are presented in Fig. 5. The resulting activation energies obtained from this method are listed in Table 1. The average value of E_a for the ignition of Mg/

NaNO₃ mixture was $148.46 \pm 3.37 \text{ kJ mol}^{-1}$, which is very close to the result of Ostmark and Roman (148 kJ mol^{-1}) [17].

It is clear from Table 1 that the activation energy has a little variation with α . The value of E_a is considered to be independent of α , if the relative error of the E_a calculated from isoconversional method is less than 10 %. In addition, the single-step reaction mechanism will be dominated when E_a is independent of α [32]. The difference between maximum and minimum values of E_a is about 6.5 % of the average E_a , indicating that the value of E_a remained approximately constant and independent of α . So the ignition process occurs through a single-step mechanism.

Determination of the kinetic triplet by model fitting method

The kinetic parameters strongly depend on selection of a proper mechanism function for the process. Therefore, determination of the most probable mechanism function is highly essential. To determine the reaction model for ignition of Mg/NaNO₃ pyrotechnic, 25 different kinetic

Table 2 Twenty-five types of mechanism functions $g(\alpha)$ and $f(\alpha)$ used to describe the solid-state reactions [31, 32]

No.	Symbol	Mechanism function name	$g(\alpha)$	$f(\alpha)$
1	$F_{1/3}$	One-third order	$1-(1-\alpha)^{2/3}$	$3/2(1-\alpha)^{1/3}$
2	$F_{3/4}$	Three-quarters order	$1-(1-\alpha)^{1/4}$	$4(1-\alpha)^{3/4}$
3	$F_{3/2}$	One and a half order	$(1-\alpha)^{-1/2}-1$	$2(1-\alpha)^{3/2}$
4	F_2	Second order	$(1-\alpha)^{-1}-1$	$(1-\alpha)^2$
5	F_3	Third order	$(1-\alpha)^{-2}-1$	$1/2(1-\alpha)^3$
6	$P_{3/2}$	Mampel power law	$\alpha^{3/2}$	$(2/3)\alpha^{-1/2}$
7	$P_{1/2}$	Mampel power law	$\alpha^{1/2}$	$2\alpha^{1/2}$
8	$P_{1/3}$	Mampel power law	$\alpha^{1/3}$	$3\alpha^{2/3}$
9	$P_{1/4}$	Mampel power law	$\alpha^{1/4}$	$4\alpha^{3/4}$
10	A_1, F_1	Avrami–Erofeev equation	$-\ln(1-\alpha)$	$(1-\alpha)$
11	$A_{3/2}$	Avrami–Erofeev equation	$[-\ln(1-\alpha)]^{2/3}$	$3/2(1-\alpha)[- \ln(1-\alpha)]^{1/3}$
12	A_2	Avrami–Erofeev equation	$[-\ln(1-\alpha)]^{1/2}$	$2(1-\alpha)[- \ln(1-\alpha)]^{1/2}$
13	A_3	Avrami–Erofeev equation	$[-\ln(1-\alpha)]^{1/3}$	$3(1-\alpha)[- \ln(1-\alpha)]^{2/3}$
14	A_4	Avrami–Erofeev equation	$[-\ln(1-\alpha)]^{1/4}$	$4(1-\alpha)[- \ln(1-\alpha)]^{3/4}$
15	F_0, R_1	Power law	α	$(1-\alpha)^0$
16	$F_{1/2}, R_2$	Power law	$1-(1-\alpha)^{1/2}$	$2(1-\alpha)^{1/2}$
17	$F_{2/3}, R_3$	Power law	$1-(1-\alpha)^{1/3}$	$3(1-\alpha)^{2/3}$
18	D_1	Parabola law	α^2	$1/2\alpha$
19	D_2	Valensi equation	$\alpha+(1-\alpha)\ln(1-\alpha)$	$[-\ln(1-\alpha)]^{-1}$
20	D_3	Jander equation	$[1-(1-\alpha)^{1/3}]^2$	$3/2(1-\alpha)^{2/3}[1-(1-\alpha)^{1/3}]^{-1}$
21	D_4	Ginstling–Brounstein equation	$1-2\alpha/3-(1-\alpha)^{2/3}$	$3/2[(1-\alpha)^{-1/3}-1]^{-1}$
22	D_5	Zhuravlev, Lesokin, Tampelman equation	$[(1-\alpha)^{-1/3}-1]^2$	$3/2(1-\alpha)^{4/3}[(1-\alpha)^{-1/3}-1]^{-1}$
23	D_6	Anti-Jander equation	$[(1+\alpha)^{1/3}-1]^2$	$3/2(1+\alpha)^{2/3}[(1+\alpha)^{1/3}-1]^{-1}$
24	D_7	Anti-Ginstling–Brounstein equation	$1+2\alpha/3-(1+\alpha)^{2/3}$	$3/2[(1+\alpha)^{-1/3}-1]^{-1}$
25	D_8	Anti-Zhuravlev, Lesokin, Tampelman equation	$[(1+\alpha)^{-1/3}-1]^2$	$3/2(1+\alpha)^{4/3}[(1+\alpha)^{-1/3}-1]^{-1}$

functions of the common models in solid-state reactions (listed in Table 2 [33, 34]) were tested with the two model fitting, differential Eq. (6) and integral Eq. (7) methods listed as following [35]: Differential method:

$$\ln \left[\frac{d\alpha/dT}{f(\alpha) \left[\frac{E_a(T-T_0)}{RT^2+1} \right]} \right] = -\frac{E_a}{RT} + \ln \left[\frac{A}{\beta} \right]. \quad (6)$$

Integral equation:

$$\ln \left[\frac{g(\alpha)}{T-T_0} \right] = -\frac{E_a}{RT} + \ln \left[\frac{A}{\beta} \right]. \quad (7)$$

According to the above-mentioned equations, the plots of $\ln[(d\alpha/dT)/f(\alpha)(E_a(T-T_0)/RT^2+1)]$ versus $1/T$ and $\ln[g(\alpha)/(T-T_0)]$ versus $1/T$ at different heating rates (β_s) can be obtained by linear regression. The function $g(\alpha)$ is the most probable mechanism function, which affords the most linear plot with a linear regression coefficient R^2 closest to -1.000 .

For accurate determination of the reaction model and pre-exponential factor, the compensation effect was used

Table 3 The kinetic triplet of the Mg/NaNO₃ ignition reaction obtained using model fitting method

$\beta/$ °C min ⁻¹	Mechanism function, $g(\alpha)$	$E_a/\text{kJ mol}^{-1}$	$\ln A/\text{min}^{-1}$	R^2
5	$[-\ln(1-\alpha)]^{1/4}$	125.11 ± 6.28	18.79 ± 1.37	0.960
10		119.32 ± 5.79	17.88 ± 1.75	0.964
15		129.25 ± 2.88	19.76 ± 0.52	0.990
20		127.80 ± 4.8	19.28 ± 0.87	0.996

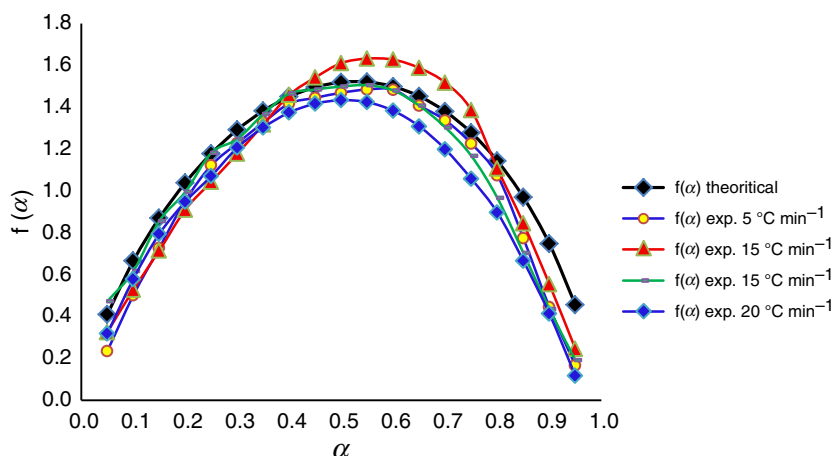
[20] and the obtained E_i and A_i values from each of the models at different heating rates were replaced in Eq. (8) to determine the compensation effect parameters a and b .

$$\ln A_i = aE_i + b. \quad (8)$$

The pre-exponential factor A_0 was calculated by substitution of the obtained E_0 from the model-free method and the a and b parameters in Eq. (9):

$$\ln A_0 = aE_0 + b. \quad (9)$$

Fig. 6 The plots of theoretical and experimental $f(\alpha)$ against various conversions ($\alpha = 0.05$ – 0.95 , with 0.05 increment) at different heating rates



The obtained results are presented in Table 3. The E_o and A_o values were substituted into Eq. (10).

$$f(\alpha) = \beta \left(\frac{d\alpha}{dT} \right)_{\alpha} \left[A_o e^{\left(\frac{-E_o}{RT\alpha} \right)} \right]^{-1}. \quad (10)$$

The calculated numerical values of $f(\alpha)$ were compared against the theoretical dependencies obtained from the $f(\alpha)$ equations (e.g., Table 2) in order to identify the best matching model.

When this method was applied for all of the reaction models, the mechanism function 14 appeared as the best pattern because of the minimum difference between experimental and theoretical data. Therefore, Avrami–Erofeev A_4 model can be selected as the most probable model and verified by sigmoidal curves of α – T represented in Fig. 4. The plots of theoretical and experimental $f(\alpha)$ versus α at different heating rates are presented in Fig. 6.

By means of nonlinear regression method, the difference between theoretical and experimental $f(\alpha)$ was calculated through the residual sum of square (RSS) that should be minimum according to Eq. (11):

$$RSS = \sum \left(f(\alpha)_{\text{exp.}} - f(\alpha)_{\text{theor.}} \right)^2 = \text{minimum}. \quad (11)$$

The RSS values were 0.32, 0.24, 0.23, and 0.52 for heating rates of 5, 10, 15, and 20 °C min^{−1}, respectively, showing slight difference between experimental and theoretical $f(\alpha)$ and to verify the chosen reaction model. The selected model shows nucleation reaction mechanism for the ignition reaction of Mg/NaNO₃ mixture. So, it can be concluded that the mechanism function with the integral form $g(\alpha) = [-\ln(1-\alpha)]^{1/4}$ describes the Mg/NaNO₃ ignition reaction.

Conclusions

Thermal behavior of the Mg/NaNO₃ binary pyrotechnic mixture (50–50) was studied by simultaneous TG/DSC

method. An exothermic ignition peak was observed with the following characteristics with increasing heating rate: (i) shift of the T_m peak to higher temperatures, and (ii) decrease of the heat of reaction. Also, from the TG curves a mass gain was observed after the ignition point. Thus, incomplete reaction between Mg and NaNO₃ was observed which increased with the increasing heating rate.

The Starink model-free method was used to determine the activation energy (E_a) for the ignition reaction. The mean value of the activation energy for α in the range of 0.1–0.9 was 148.46 kJ mol^{−1} using these methods. The difference between the maximum and minimum values of E_a is about 6.5 % of the average E_a . This result indicates that the value of E_a is independent of α , and the ignition process occurs through a single-step mechanism.

The pre-exponential factor (A) and kinetic model function were determined by compensation effect that associates model-free and model fitting data to selection of the best model. By this method, a nucleation reaction model (A_4 model) was assigned to the mechanism of the ignition reaction and the selected model was verified by nonlinear model fitting method.

Acknowledgements We would like to thank the research committee of Malek-ashtar University of Technology (MUT) and Professor M. K. Amini for supporting this work.

References

- Conkling JA. Chemistry of pyrotechnics: basic principles and theory. New York: Marcel Dekker Inc.; 1985.
- De Klerk WPC, Colpa W, Ekeren PJ. Ageing studies of magnesium-sodium nitrate pyrotechnic compositions. J Therm Anal Calorim. 2006;85:203–7.
- Brown SD, Charsley EL, Goodall SJ, Laye PG, Rooney JJ, Griffiths TT. Studies on the ageing of a pyrotechnic composition using isothermal heat flow calorimetry and thermal analysis techniques. Thermochim Acta. 2003;401:53–61.
- Redkar AS, Mujumdar VA, Singh SN. Study on magnesium based pyrotechnic composition as a priming charge. Def Sci J. 1996;46:41–7.

5. Pourmortazavi SM, Hajimirsadeghi SS, Kohsari I, Fathollahi M, Hosseini SG. Thermal decomposition of pyrotechnic mixtures containing either aluminum or magnesium powder as fuel. *Fuel*. 2008;87:244–51.
6. Kang X, Zhang J, Zhang Q, Du K, Tang Y. Studies on ignition and afterburning processes of KClO_4/Mg pyrotechnics heated in air. *J Therm Anal Calorim*. 2012;109:1333–40.
7. Zhu CG, Wang HZ, Min L. Ignition temperature of magnesium powder and pyrotechnic composition. *J Energ Mater*. 2014;32: 219–26.
8. Musanic SM, Houra IF, Sucasca M. Applicability of non-isothermal DSC and Ozawa method for studying kinetics of double base propellant decomposition. *Cent Eur J Energ Mater*. 2010;7: 233–51.
9. Moghaddam AZ, Rees GJ. Thermoanalytical studies on pyrotechnic reactions. *Scientia Iranica*. 2003;10:267–72.
10. Chiu MH, Prenner EJ. Differential scanning calorimetry: an invaluable tool for a detailed thermodynamic characterization of macromolecules and their interactions. *J Pharm Bioallied Sci*. 2011;3:39–59.
11. Miao Y, Liping Ch, Jinyang Y, Jinhua P. International symposium on safety science and technology thermoanalytical investigation on pyrotechnic mixtures containing Mg–Al alloy powder and barium nitrate. *Proc Eng*. 2012;45:567–73.
12. Vyazovkin S, Wight CA. Model-free and model-fitting approaches to kinetic analysis of isothermal and nonisothermal data. *Thermochim Acta*. 1999;340–341:53–68.
13. Chen G, Lee Ch, Kuo Y, Yen YW. A DSC study on the kinetics of disproportionation reaction of $(\text{hfac})\text{CuI}(\text{COD})$. *Thermochim Acta*. 2007;456:89–93.
14. Ribeiro B, Nohara L, Oishi S, Costa M, Botelho E. Nonoxidative thermal degradation kinetic of polyamide 6,6 reinforced with carbon nanotubes. *J Thermoplast Compos Mater*. 2013;26: 1317–31.
15. Yunqing H, Haixiang Ch, Naian L. New incremental isoconversional method for kinetic analysis of solid thermal decomposition. *J Therm Anal Calorim*. 2011;104:679–83.
16. Jankovic B, Mentus S, Jankovic M. A kinetic study of the thermal decomposition process of potassium metabisulfite: estimation of distributed reactivity model. *J Phys Chem Solids*. 2008;69: 1923–33.
17. Ostmark H, Roman N. Laser ignition of pyrotechnic mixtures: ignition mechanisms. *J Appl Phys*. 1993;73:1993–2003.
18. Rao RB, Singh H. Burning rate characteristics of Mg– NaNO_3 propellants. *Def Sci J*. 1992;42:173–6.
19. Palaiah RS, Joshi PH, Deo SS, Jawale DK, Valiv MH, Somayajulu MR. Luminous efficient compositions based on epoxy resin. *Def Sci J*. 2006;56:339–43.
20. Vyazovkin S, Burnham AK, Criado JM, Pérez-Maqueda LA, Popescu C, Sbirrazzuoli N. ICTAC Kinetics Committee recommendations for performing kinetic computations on thermal analysis data. *Thermochim Acta*. 2011;520:1–19.
21. Bauer T, Laing D, Kröner U, Tamme R. Sodium nitrate for high temperature latent storage. In: *The 11th international conference on thermal energy storage in stockholm*, 2009.
22. Conking JA, Mocella CJ. *Chemistry of pyrotechnics basic principles and theory*. New York: Taylor and Francis Group Inc.; 2011.
23. Chunmiao Y, Lifu Y, Chang L, Gang L, Shengjun Zh. Thermal analysis of magnesium reactions with nitrogen/oxygen gas mixtures. *J Hazard Mater*. 2013;260:707–14.
24. Jriri T, Rogez J, Bergman C, Mathieu JC. Thermodynamic study of the condensed phases of NaNO_3 , KNO_3 , and CsNO_3 , and their transitions. *Thermochim Acta*. 1995;266:147–61.
25. Hussain G, Rees GJ. A study on combustion behavior of carbon–sulphur–sodium nitrate mixture. *J Therm Anal Calorim*. 1991;37: 757–62.
26. Akbar J, Iqbal MS, Massey Sh, Masih R. Kinetics and mechanism of thermal degradation of pentose—and hexose—based carbohydrate polymers. *Carbohydr Polym*. 2012;90:1386–93.
27. Fernandez d’Arlas B, Rueda L, Stefani PM, de la Caba K, Mondragon I, Eceiza A. Kinetic and thermodynamic studies of the formation of a polyurethane based on 1,6-hexamethylene diisocyanate and poly(carbonate-co-ester) diol. *Thermochimica Acta*. 2007;459:94–103.
28. Vyazovkin S, Wight CA. Isothermal and non-isothermal kinetics of thermally stimulated reactions of solids. *Int Rev Phys Chem*. 1998;17:407–33.
29. Pouretdal HR, Ebadpour R. Application of non-isothermal thermogravimetric method to interpret the decomposition kinetics of NaNO_3 , KNO_3 , and KClO_4 . *Int J Thermophys*. 2014;35: 942–51.
30. Georgieva V, Zvezdova D, Vlaev L. Non-isothermal kinetics of thermal degradation of chitosan. *Chem Cent J*. 2012;6:1–10.
31. Starink MJ. The determination of activation energy from linear heating rate experiments: a comparison of the accuracy of isoconversion methods. *Thermochim Acta*. 2003;404:163–76.
32. Ram IS, Singh K. Study of crystallization process in $\text{Se}_{80}\text{In}_{10}\text{Pb}_{10}$ by iso-conversional methods. *J Cryst Process Technol*. 2013;3:49–55.
33. Noisong P, Danvirutai C. Kinetics and mechanism of thermal dehydration of $\text{KMnPO}_4 \cdot \text{H}_2\text{O}$ in a nitrogen atmosphere. *Ind Eng Chem Res*. 2010;49:3146–51.
34. Pouretdal HR, Damiri S, Ghaemi EF. Non-isothermal studies on the thermal decomposition of C4 explosive using the TG/DTA technique. *Cent Eur J Energ Mater*. 2014;11:285–94.
35. Feng-Qi Zh, Rong-Zu H, Pei Ch, Yang L, Sheng-Lib G, Ji-Rong S, Qi-Zhen Sh. Kinetics and mechanism of the exothermic first-stage decomposition reaction of dinitroglycoluril. *Chin J Chem*. 2004;22:649–52.